Effects of Crosslinking on Thermal and Mechanical Properties of Polyurethanes

BOR-SEN CHIOU, PAUL E. SCHOEN

Center for Bio/Molecular Science and Engineering, Naval Research Laboratory, Washington, D.C. 20375

Received 7 December 2000; accepted 13 April 2001

ABSTRACT: The effects of chemical crosslinking on the thermal and dynamic mechanical properties of a polyurethane system were examined. The polyurethanes were prepared from poly(propylene glycol), a diol; trimethylolpropane propoxylate, a triol; and poly(propylene glycol), tolylene 2,4-diisocyanate terminated, a diisocyanate monomer. The crosslink density was controlled by varying the triol concentration from 10 to 70 mol % and the isocyanate-to-hydroxyl (NCO/OH) ratio from 1.0 to 1.3. All the samples had one glass-transition temperature and no crystalline regions. In addition, there were larger increases in glass-transition temperature over the range of triol concentrations studied than over the range of NCO/OH ratios studied. For all samples, the Dibenedetto equation relating glass-transition temperature to extent of crosslinking fit the data very well. Also, samples with higher crosslink densities had much larger elastic moduli for temperatures above the glass-transition temperature. By assuming the system was a phantom network, approximate crosslink densities for stoichiometric samples were obtained from the dynamic mechanical data and these agreed fairly well with theoretical predictions. © 2002 John Wiley & Sons, Inc. J Appl Polym Sci 83: 212–223, 2002

Key words: polyurethane; glass-transition temperature; crosslink density

INTRODUCTION

Polyurethane elastomers have a wide range of material properties attributed to the large variety of possible morphologies that may exist in the polymers. These morphologies are partly controlled by the presence of physical and chemical crosslinks. In some systems, both types of crosslinks may be present. Physical crosslinking occurs by hydrogen bonding and hard domain formation. Domain formation develops because the soft segments consisting of the polyols are incompatible with the hard segments containing the diisocyanate part. These two types of segments phase separate and hydrogen bonding may occur between or within the segments. The hard segments act as both physical crosslinks and fillers.[1] In some cases, crystalline regions may form in the hard and soft domains. Chemical crosslinking can be introduced into the system in many ways, but common methods include using a triol or higher-functional polyol and having the isocyanate-to-hydroxyl (NCO/OH) ratio greater than 1. In these nonstoichiometric samples, the excess isocyanate groups react with urethane groups to form allophanate linkages.[1]

Various studies have examined the effects of chemical crosslinking on the material properties of polyurethane elastomers. Many of these studies have focused on the tensile properties of the polymers.[2–13] In addition, the effects of crosslinking on swelling,[2,3,5,8,9,11–13] thermal degradation,[6,10,12] thermal properties,[5,9–12] and morphology[10,12,13] have been examined. The chemical crosslinks have been introduced into the samples

Correspondence to: B.-S. Chiou (bsc@cbmse.nrl.navy.mil).
Contract grant sponsor: Office of Naval Research.

Journal of Applied Polymer Science, Vol. 83, 212–223 (2002)

in a variety of ways. Some systems contain triols or higher-functional polyols,[2–7,12] isocyanates with functionalities greater than two,[8,11] NCO/OH ratios greater than 1,[4,6,7,9,12] or combinations thereof.[4,6,7,12]

In this study we characterize the effects of chemical crosslinking on the thermal and dynamic mechanical properties of a polyurethane system. The polyurethane is to be used as the matrix for tubule composites, and is prepared from a diol, a triol, and a diisocyanate monomer. We controlled the crosslink density by varying the triol concentration and the NCO/OH ratio in the system. We focus on examining the effects of crosslinking on the glass-transition temperature and the elastic modulus of the samples.

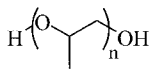

Poly(propylene glycol)

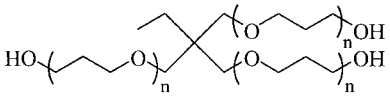

Trimethylolpropane Propoxylate

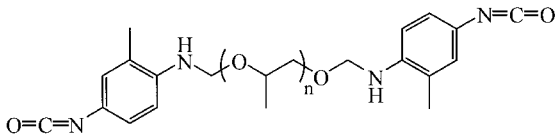

Poly(propylene glycol), tolylene 2,4-diisocyanate terminated

Figure 1 Chemical structures of the diol, triol, and diisocyanate monomer.

EXPERIMENTAL

Sample Preparation

The polyurethane formulations were prepared from a diol, a triol, and a diisocyanate monomer. The diol was poly(propylene glycol), with a molecular weight of 425, and the triol was trimethylolpropane propoxylate, with a molecular weight of 308. Both alcohols were dried by heating them at 60°C in a vacuum oven. Poly(propylene glycol) was dried for 5 h, whereas trimethylolpropane propoxylate was dried for 3 h. The diisocyanate monomer used was poly(propylene glycol), tolylene 2,4-diisocyanate terminated, with a molecular weight of 1000. It was used as received. Both the alcohols and the diisocyanate monomer were obtained from Sigma–Aldrich (St. Louis, MO). Their chemical structures are shown in Figure 1. The crosslink density of the samples can be controlled by varying the triol concentration and the NCO/OH ratio. The triol concentration was varied from 10 to 70 mol % of the total hydroxyl groups, whereas the NCO/OH ratio was varied from 1.0 to 1.3. In addition to the monomers, the formulations contained a catalyst, dibutyltin dilaurate; a plasticizer, dibutyl adipate; and a commercial antifoaming agent, AF-4. The concentrations of catalyst, plasticizer, and antifoaming agent were 0.50, 2.0, and 0.30 wt %, respectively. All concentrations were based on the weight of the monomers. The AF-4 was obtained from BJB Enterprises (Tustin, CA); the catalyst and plasticizer were obtained from Sigma–Aldrich.

The formulations were prepared by the one-shot method, where all the ingredients were mixed together at once and allowed to cure. The samples were vigorously stirred by hand for several minutes and then placed in polystyrene weighing dishes. Each dish was coated with a silicone release agent (Ease Release 400; BJB Enterprises), so that the sample could be readily separated from the dish. The samples were then degassed in a vacuum oven at 25°C for several hours. They were taken out of the oven and cured in the atmosphere for at least 2 days. Finally, the samples were placed back in the oven and cured at 60°C for an additional 24 h.

Differential Scanning Calorimetry

A Perkin–Elmer differential scanning calorimeter (DSC 7; Perkin Elmer Cetus Instruments, Norwalk, CT) was used to determine the thermal transitions of the polyurethane samples. Samples weighing approximately 20 mg were scanned at a rate of 10°C/min from −60 to 90°C. The samples remained in a nitrogen atmosphere during the course of the experiments. Two scans were performed for each sample with the second scan used in the data analysis.

Dynamic Mechanical Analysis

A TA Instruments dynamic mechanical analyzer (DMA 2980; TA Instruments, New Castle, DE) was used to measure the dynamic mechanical properties of the samples. The samples were cut into 10-mm-wide by 4-mm-thick strips and placed in a 35-mm-long dual cantilever. A temperature ramp test was

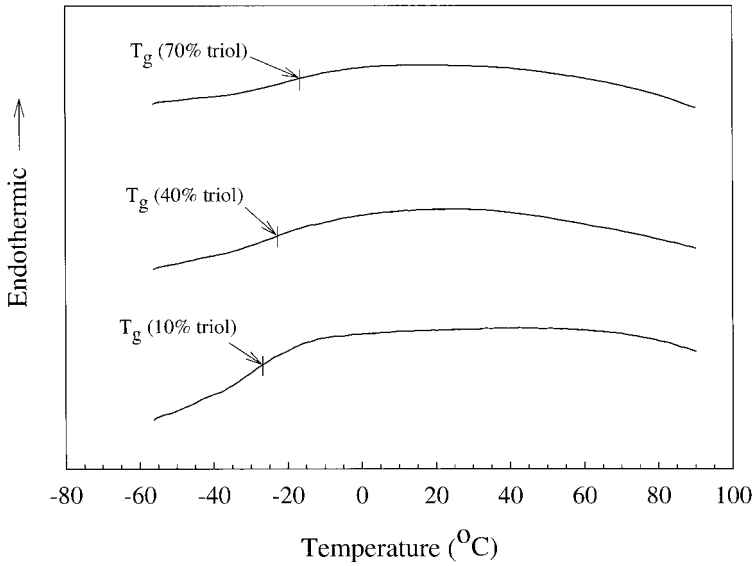

Figure 2 Three DSC scans for samples with an NCO/OH ratio of 1.0 and three triol concentrations.

performed to determine the elastic modulus E' and the viscous modulus E'', for a temperature range of −110 to 70°C. The frequency of the test was 1 Hz and the temperature scanning rate was 2°C/min. The elastic modulus measures the amount of energy stored per oscillation cycle, whereas the viscous modulus measures the amount of energy dissipated per cycle. For stoichiometric samples, the temperature range was extended to 105°C to determine the plateau modulus.

Fourier Transform Infrared Spectroscopy

A Nicolet Magna 750 Fourier transform infrared (FTIR) spectrometer (Nicolet Instruments, Madison, WI) with a DTGS-KBR detector was used to monitor the polyurethane reaction. The precure formulation was sandwiched between two BaF_2 crystals along with a 50-μm Teflon spacer. The sample was allowed to cure in air for several days. It was then placed in an oven and cured at 60°C for 24 h. The asymmetric stretching vibration of the NCO group at 2270 cm^{-1} was used to determine the completeness of the cure.

RESULTS AND DISCUSSION

Effects of Crosslinking on Glass-Transition Temperature

All the polyurethane samples exhibited one glass-transition temperature (T_g) over the temperature range studied. Figure 2 shows three representative DSC scans for samples with an NCO/OH ratio of 1.0 and various triol concentrations. The single T_g for each sample suggests that there may not be any phase separation into soft and hard domains, which occurs for other polyurethane elastomers.[1] In addition, no endothermic peaks appear in the scans, indicating that crystalline regions do not exist in our samples. Both phase separation and crystalline formation may have been inhibited by the presence of chemical crosslinks. The DSC scans also show that as the concentration of triol increases, the glass-transition shifts to higher temperatures. This is attributed to the increase in crosslink density that restricts the molecular motion of the polymer chains and leads to the increase in T_g.

The glass-transition temperatures increased for higher triol concentrations and larger NCO/OH ratios. This is shown in Figure 3 where we plot the samples' T_g's as a function of triol concentration for various NCO/OH ratios. The glass-transition temperature increased about 7–11°C for an increase in the triol concentration from 10 to 70 mol %. Similarly, the T_g's increased about 2–5°C for an increase in NCO/OH ratio from 1.0 to 1.3. This seems to indicate that we examined a wider range of crosslink densities when we varied the triol concentration from 10 to 70 mol % than when we varied the NCO/OH ratio from 1.0 to 1.3. In fact, the incremental increase in T_g obtained by varying NCO/OH from 1.0 to 1.3 corresponded to approximately the same increase in T_g found by varying triol concentration from 10

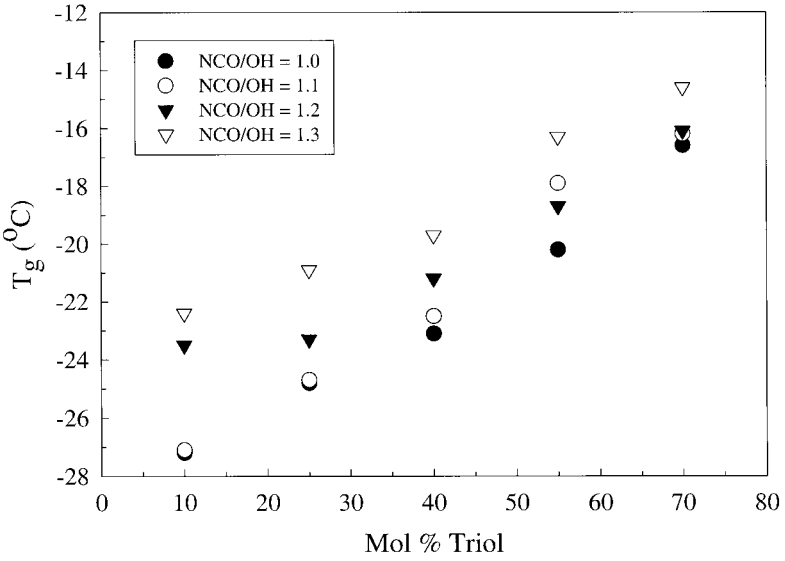

Figure 3 Glass-transition temperatures (T_g's) as a function of triol concentration for various NCO/OH ratios. The standard deviations generally lie between 0.5 and 1.0°C.

to 40 mol %. However, direct comparison of T_g and crosslink density between stoichiometric and nonstoichiometric samples may not be appropriate. In nonstoichiometric samples, excess diisocyanates react with urethane groups to form allophanate linkages,[1] which may not be present in stoichiometric samples. Therefore, in addition to the crosslink density, the effect of allophanate groups on T_g for nonstoichiometric samples needs to be considered before comparisons can be made.

Various theories have been proposed to account for the effects of crosslinking on the glass-transition temperature of polymers.[14–17] One such theory resulted in Dibenedetto's equation relating glass-transition temperature and extent of crosslinking[14]:

$$\frac{T_g - T_{g0}}{T_{g0}} = \frac{\left(\frac{E_x}{E_m} - \frac{F_x}{F_m}\right)X_c}{1 - \left(1 - \frac{F_x}{F_m}\right)X_c} \qquad (1)$$

where T_g (K) is the glass-transition temperature; T_{g0} (K) is the glass-transition temperature of a polymer with the same chemical composition as the crosslinked polymer, but without the crosslinks; E_x/E_m is the ratio of the lattice energies for crosslinked and noncrosslinked polymers; F_x/F_m is the ratio of the segmental mobilities of the crosslinked and noncrosslinked polymers; and X_c is the mole fraction of monomer units that are crosslinked in the polymer. The copolymer effect on T_g ascribed to the crosslinking agent has been accounted for in T_{g0}, so eq. (1) predicts only the shift in T_g associated with crosslinking. For most polymers, the mobility of crosslinked units is essentially zero, so F_x/F_m can be set equal to zero.[14] Rearranging eq. (1), we obtain

$$T_g = KT_{g0}\frac{X_c}{1 - X_c} + T_{g0} \qquad (2)$$

where K contains the lattice energy terms. A plot of T_g as a function of $X_c/(1 - X_c)$ should result in a straight line. Such a plot for all samples is shown in Figure 4. We determine X_c in the stoichiometric samples by calculating the mole fraction of triol crosslinkers and in the nonstoichiometric samples by assuming all the excess diisocyanate monomers become crosslinkers. In these calculations, we assume complete conversion of the reactants. The data for all samples indicate a good fit to the Dibenedetto equation. The assumption that complete conversion of reactants occurred may not be entirely accurate, although FTIR data do show that the samples achieved very high conversions. The FTIR spectra, shown in Figure 5 for a sample (70 mol % triol with NCO/OH = 1.3) before and after curing, indicated that most of the diisocyanate groups reacted during the polymerization. The isocyanate (NCO) group at 2270 cm^{-1} has a large absorbance before curing, but decreases to almost zero absorbance after curing. In addition to incomplete conversion

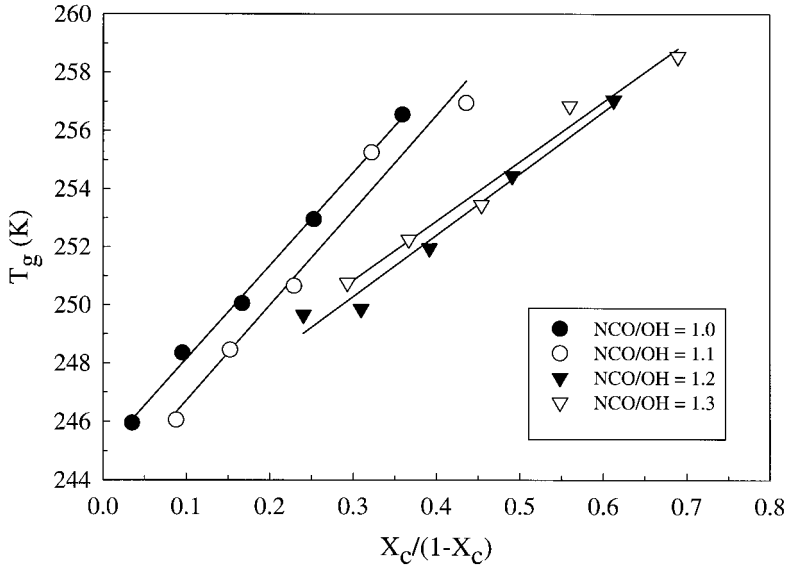

Figure 4 Dibenedetto plot for all the samples. The data for samples with NCO/OH ratios of 1.2 and 1.3 have been shifted along the *x*-axis by 0.1 to make the plot clearer.

of reactants, possible side reactions, such as the reaction of diisocyanate with moisture in the air, might have occurred. However, these factors do not appear to have a significant effect on the Dibenedetto plot.

Effects of Crosslinking on Dynamic Mechanical Properties

The polyurethane samples display dynamic mechanical behavior characteristic of elastomers. The samples' glass-transition temperatures are below room temperature and their elastic moduli eventually reach a plateau at higher temperatures. Figure 6 shows the dynamic mechanical behavior of a typical sample with a plot of the elastic modulus (E'), viscous modulus (E''), and loss tangent (E''/E') as a function of temperature. In this case, the sample contains 10 mol % triol and has an NCO/OH ratio of 1.1. At temperatures below its glass transition, the elastic modulus remains relatively constant and is more than an

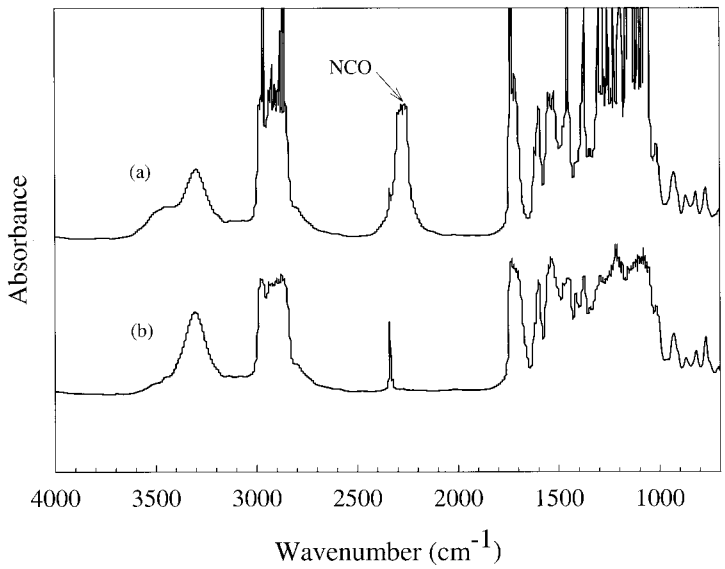

Figure 5 FTIR spectra showing (a) precure and (b) fully cured sample containing 70 mol % triol with an NCO/OH ratio of 1.3. The asymmetric stretching vibration of the NCO group at 2270 cm^{-1} is used to monitor the polyurethane reaction.

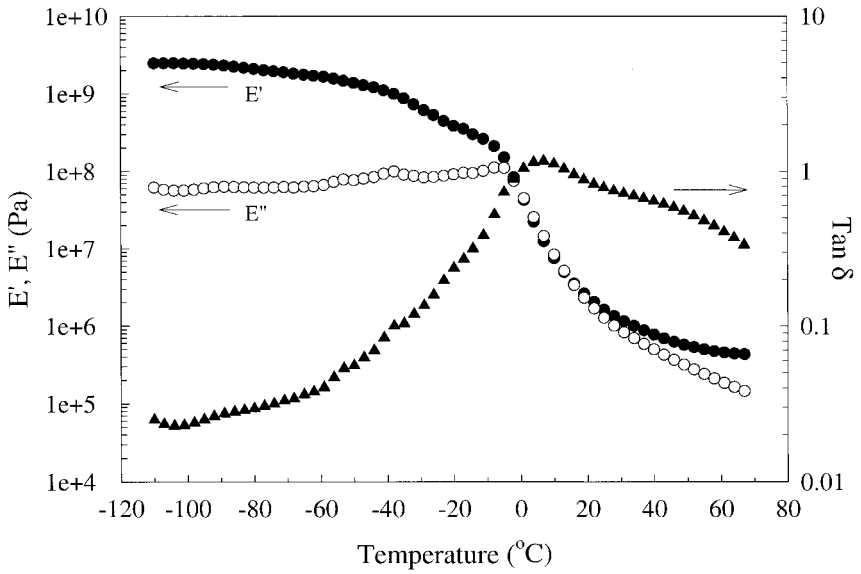

Figure 6 Representative dynamic mechanical data showing elastic modulus (E'), viscous modulus (E''), and loss tangent (tan δ) as a function of temperature. The sample contains 10 mol % triol and has an NCO/OH ratio of 1.1.

order of magnitude greater than the viscous modulus. Once the glass-transition temperature is reached, the elastic modulus decreases rapidly as the polymer chains begin to move. The elastic modulus continues to decrease until it plateaus at around 60°C. At this point, the chemical crosslinks prevent the polymer from flowing. The loss tangent maximum is usually used to determine the glass-transition temperature. However, for our samples, the maxima occur at much higher temperatures than the glass-transition temperatures determined by DSC. The viscous modulus maximum was also used as a measure of glass transition. For our samples, these maxima always appear at lower temperatures than the loss tangent maxima, but still remain about 20–25°C greater than the glass-transition temperatures obtained from DSC.

The crosslink density of the polyurethane samples has a pronounced effect on the elastic modulus at temperatures greater than the glass-transition temperature. This is shown in Figure 7, where we plot the elastic moduli as a function of temperature for samples with an NCO/OH ratio of 1.2 and various triol concentrations. All the other samples with constant NCO/OH ratios and varying triol concentrations behave in a similar manner, so we show only this representative plot. Below the glass-transition temperature, all the samples have an elastic modulus of approximately 2×10^9 Pa. Once the glass-transition temperature is reached, the modulus begins to decrease rapidly. The modulus for samples with lower crosslink density decreases at a lower temperature and at a faster rate than the samples with higher crosslink density. At even higher temperatures, the modulus continues to diverge. Over certain temperature ranges, the modulus for the 70 mol % triol sample becomes more than an order of magnitude greater than the modulus for the 10 mol % triol sample.

When we varied the NCO/OH ratio instead of the triol concentration, the differences in elastic modulus values became smaller. This is shown in Figure 8, where we plot the elastic modulus as a function of temperature for samples with 55 mol % triol and various NCO/OH ratios. The other samples with constant triol concentrations and varying NCO/OH ratios behaved in a similar manner so we show only this representative plot. The elastic modulus curves follow the same trends as those shown in Figure 7. However, the largest differences in modulus values over the range of NCO/OH ratios studied were smaller than those found over the range of triol concentrations studied. This indicates that varying the NCO/OH ratios results in smaller crosslink density variations. This agrees with the DSC data, where we found larger differences in T_g among the samples with varying triol concentrations.

We can also determine how varying the triol concentration and the NCO/OH ratio affects the samples' network structures by examining their loss tangents. Figure 9 shows the loss tangents

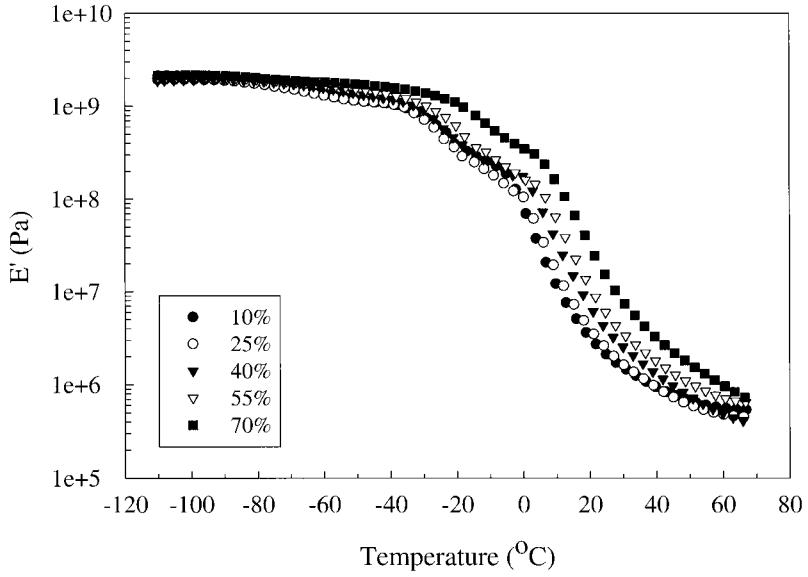

Figure 7 Elastic modulus as a function of temperature for samples having an NCO/OH ratio of 1.2 with varying triol concentrations.

for different triol concentrations [Fig. 9(a)] and NCO/OH ratios [Fig. 9(b)] as a function of temperature. Increasing the crosslink density affects the loss tangent curves in three different ways. First, the loss tangent peaks shift to higher temperatures. This occurs because samples with higher crosslink densities have higher glass-transition temperatures. Second, the loss tangent peaks have lower values because samples with higher crosslink densities have larger elastic moduli relative to their viscous moduli. Third, the loss tangent peaks become broader. This broadening is attributed to an increase in the distribution of molecular weights between crosslinks or an increase in the heterogeneity of the network structure.[18] The samples with varying triol concentrations [Fig. 9(a)] show more pronounced effects in their loss tangent behavior than the samples with varying NCO/OH ratios [Fig. 9(b)]. Again, this is attributed to the larger crosslink

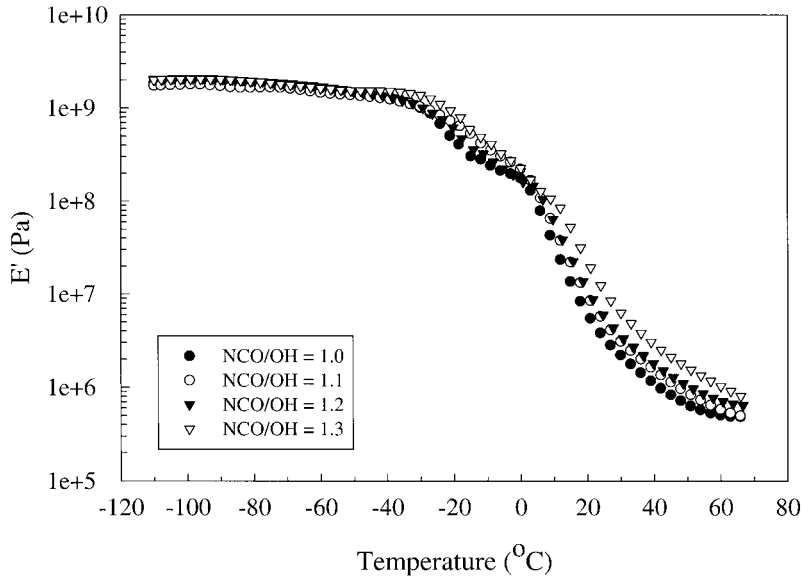

Figure 8 Elastic modulus as a function of temperature for samples containing 55 mol % triol with varying NCO/OH ratios.

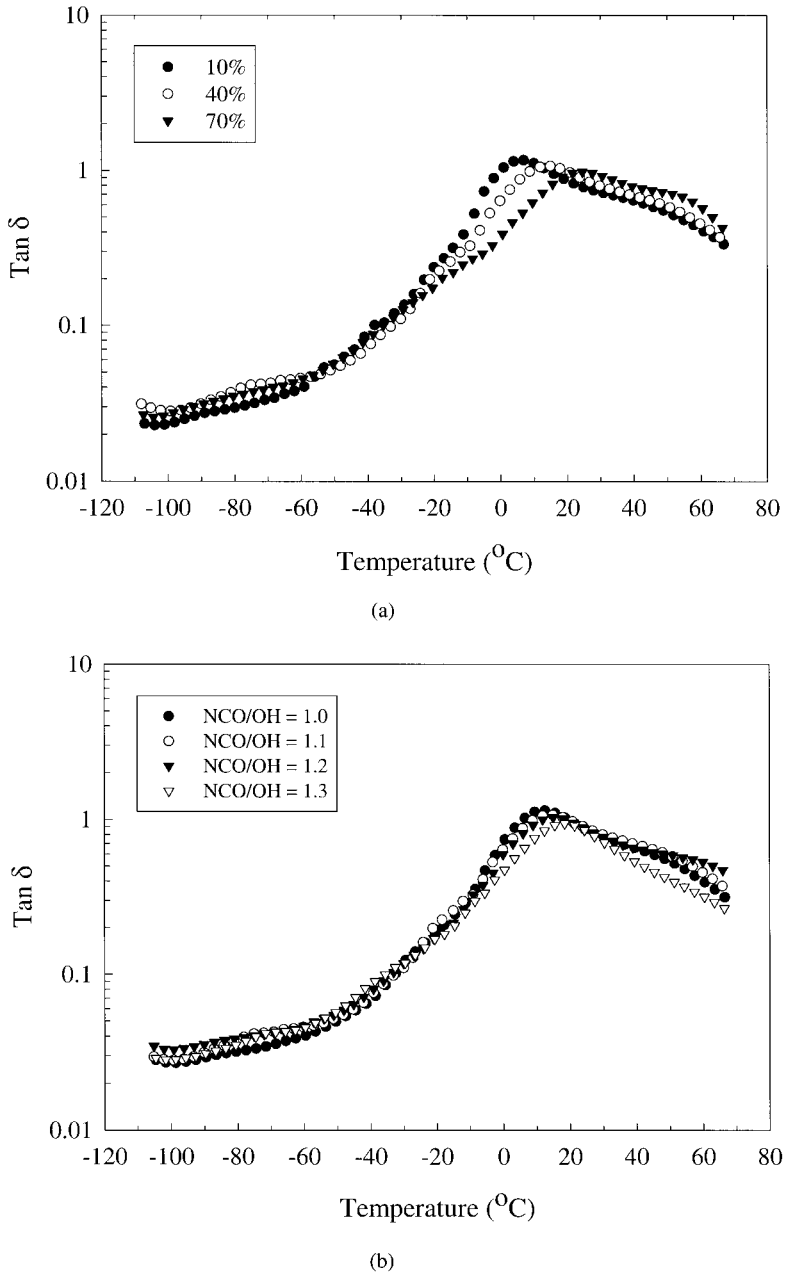

Figure 9 Loss tangents as a function of temperature for (a) constant NCO/OH ratio and (b) constant triol concentration samples. For the constant NCO/OH ratio samples, NCO/OH is 1.1. For the constant triol concentration samples, the triol concentration is 40 mol %.

density variation for the samples with varying triol concentrations.

The theoretical crosslink density for step-growth polymers, such as polyurethane in this study, can be determined by several methods. Scanlan[19,20] developed one method for ideal networks with a stoichiometric ratio of 1.0 and full conversion of reactants. Marsh et al.[21] developed another approach, which is a modification of Flory's theory on polymer networks. Unlike the Scanlan method, this approach can incorporate a nonstoichiometric ratio and incomplete conversion. It involves determining the branching coefficient, defined as the probability that an *f*-functional unit is connected via a chain of difunctional units to another *f*-functional unit. The network properties, such as crosslink density, can then be calculated from the branching coefficient and the

formulation properties. Three assumptions were made when developing this model. First, all functional groups of the same type have equal reactivities. Second, no intramolecular reactions occur in finite species. Third, all groups react independently of one another. This model has been found to work well for polyester[21] and polyurethane systems.[22,23] A third method for determining crosslink density was developed by Miller and Macosko.[24] This approach can encompass more general systems than the other two approaches. Instead of calculating the branching coefficient, this method involves determining the probability that a given branch leads to a finite chain. Material properties, such as the crosslink density, can then be determined from this probability and the formulation properties. This method also incorporates the same assumptions as those made by Marsh et al. We determined the theoretical crosslink densities for our stoichiometric samples using all three methods. In these calculations, we assume complete conversion of the reactants. A sample calculation appears in the Appendix. For stoichiometric samples at full conversion, crosslink density functions derived from the methods of both Marsh et al. and Miller and Macosko reduce to that of Scanlan's method (see Appendix).

We can obtain approximate crosslink densities of our samples from the dynamic mechanical data. To do this, we assume that the theory of rubber elasticity applies to our system. One form of this theory gives the equilibrium shear modulus G as[25,26]

$$G = (\nu - h\mu)RT \tag{3}$$

where ν is the concentration of elastically active chains, h is an empirical parameter whose values lie between 0 and 1, μ is the concentration of elastically active junctions, R is the gas constant, and T is the temperature. In a perfect network with functionality f, μ is equal to $2\nu/f$. We assume that only chemical crosslinking contributes to the modulus and neglect the contribution from physical entanglements. This assumption is valid because the monomers in our system have low molecular weights. Physical entanglements can be accounted for by adding the term $G_N^\circ T_e$ to the right side of eq. (3), where G_N° is the plateau modulus associated with physical entanglements in a nonchemically crosslinked system and T_e is the proportion of physical entanglements that is elastically active. The shear modulus from eq. (3) can be determined for a phantom network, an affine network, or anything in between. For a phantom network, junctions can fluctuate about their mean positions because of Brownian motion and h has a value of one. For an affine network, these fluctuations are completely suppressed and h has a value of zero. The network properties can be intermediate between these two types, in which case h has a value between zero and one. Our trifunctional polyurethane system should behave more like a phantom network, given that junctions move more affinely only if they have very high functionalities.[27,28] For a trifunctional phantom network ($\mu = 2\nu/3$), the shear modulus becomes

$$G = \frac{\nu}{3} RT \tag{4}$$

For isotropic materials, Young's modulus E can be related to the equilibrium shear modulus G as follows[29]:

$$E = 2G(1 + n) \tag{5}$$

where n is Poisson's ratio. For elastomers, n has a value close to 0.5.[18] We can then roughly approximate E' in the rubbery plateau region as being equal to E and solve for the crosslink density by substituting eq. (5) back into eq. (4). The crosslink density is then approximately equal to E'/RT.

The experimental crosslink densities for the stoichiometric samples agree fairly well with theoretical predictions. This is shown in Figure 10, where we plot crosslink density as a function of triol concentration. We use E' at a temperature of 100°C to determine the experimental crosslink density. In addition to calculating crosslink densities for a phantom network, we perform the same calculations for an affine network and present them in the same figure. In this case, crosslink density is equal to $E'/3RT$ and some studies of higher functional systems have shown good agreement between experimental and theoretical values.[30–32] For our samples, crosslink densities based on a phantom network appear to be closer to theoretical predictions. The fit to theory is fairly good, but disparities still exist between experiment and theory. Several factors can account for this disparity. One factor involves setting the crosslink density equal to E'/RT, which is only a rough approximation. Also, Poisson's ratio for our samples may not be exactly 0.5, contributing some errors to our calculations. Another

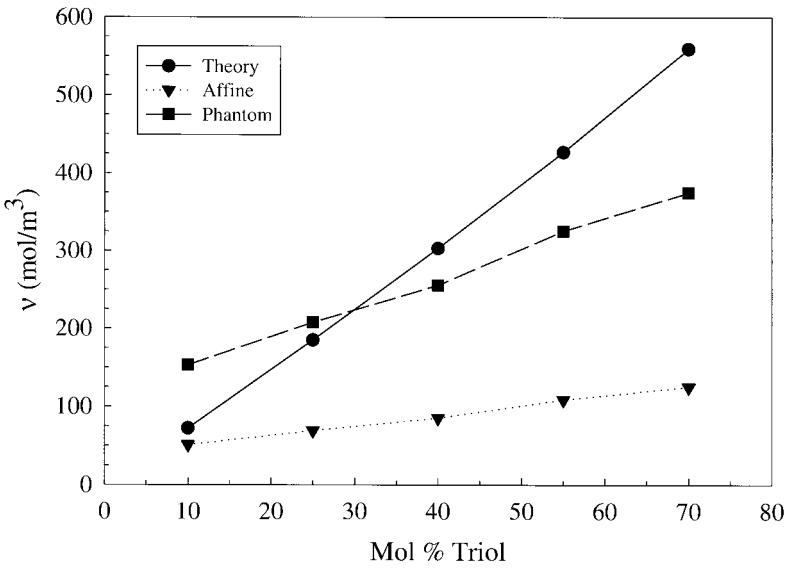

Figure 10 A comparison of experimentally determined and theoretically predicted values of crosslink density as a function of triol concentration. The data are for samples with an NCO/OH ratio of 1.0.

factor is that intramolecular and side reactions may have taken place, resulting in an imperfect network structure. In addition, a small amount of plasticizer is present in our samples, which the various theories presented here do not take into account. Both the imperfect network structure and the presence of plasticizers should result in smaller experimental crosslink densities than those predicted from theory. That is what we generally see in Figure 10.

CONCLUSIONS

All the polyurethane samples had one glass-transition temperature, indicating that phase separation did not occur. Moreover, the DSC scans showed that no crystalline regions existed in the samples. In addition, the glass-transition temperatures exhibited a larger increase over the range of triol concentrations studied than over the range of NCO/OH ratios studied. Part of this may have been because of the wider variation of crosslink densities obtained by varying the triol concentration. For all samples, the Dibenedetto equation fit the data very well.

The samples with higher triol concentrations and NCO/OH ratios had greater elastic modulus values, which is attributed to the higher crosslink densities in those samples. In addition, we examined three different theoretical models for predicting crosslink density. If we assume full conversion of reactants for the stoichiometric samples, all three models give the same results. We then compared the crosslink densities determined from the theoretical models to those obtained from the dynamic mechanical data. By assuming the polyurethane system can be described as a phantom network, the experimental crosslink densities show fairly good agreement with the theoretical predictions.

We thank the Office of Naval Research for support of this work and Dr. Robert F. Brady Jr. for helping with the polyurethane formulations.

APPENDIX

We calculated the theoretical crosslink densities for one of our polyurethane samples using methods from Scanlan,[19,20] Marsh et al.,[21] and Miller and Macosko.[24] The sample contained 40 mol % triol with an NCO/OH ratio of 1.0 and the reaction can be depicted as

$$B_2 + 0.6A_2 + 0.267A_3 \rightarrow \text{polyurethane network} \quad \text{(A.1)}$$

where B is the isocyanate group, A is the hydroxyl group, B_2 is the diisocyanate [poly(propylene glycol), tolylene 2,4-diisocyanate terminated], A_2 is the diol [poly(propylene glycol)], and A_3 is the

triol (trimethylolpropane propoxylate). For every mole of B_2, there are 0.6 mol of A_2 and 0.4(2/3) = 0.267 mol of A_3.

Method of Scanlan

The crosslink density ν was determined from[19,20]

$$\nu = \sum_{f=3}^{\infty} \frac{f}{2} C_f \tag{A.2}$$

where f is the functionality of the reactants and C_f is the concentration of reactant with functionality f, expressed as moles per volume of fully cured polymer. The functionality f is 3 or greater because species with functionalities of 2 or smaller do not form junction points in the network. For our sample, the triol was the only reactant with a functionality of 3 or greater. Therefore, we can set $f = 3$ and simplify eq. (A.2) to

$$\nu = \frac{3n_{A_3}\rho}{2(M_{B_2}n_{B_2} + M_{A_2}n_{A_2} + M_{A_3}n_{A_3})} \tag{A.3}$$

where n_{A_3} is the number of moles of A_3, n_{A_2} is the number of moles of A_2, n_{B_2} is the number of moles of B_2, M_{A_3} is the molecular weight of A_3, M_{A_2} is the molecular weight of A_2, M_{B_2} is the molecular weight of B_2, and ρ is the density of the fully cured polymer. The density for the 40 mol % triol sample is 1.01 g/cm^3. We can then solve for the crosslink density in eq. (A.3) (M_{A_3} = 308 g/mol, M_{A_2} = 425 g/mol, M_{B_2} = 1000 g/mol) and we obtain a value of 3.02×10^{-4} mol/cm^3.

Method of Marsh et al.

Marsh et al.[21] explicitly derived equations for a system containing tri-, di-, and monofunctional (A_3, A_2, and A_1) reactants with functionalities of A and di- and monofunctional (B_2 and B_1) reactants with functionalities of B. However, this method can be extended to other systems. The crosslink density can be determined from first calculating the branching coefficient α[21]:

$$\alpha = \frac{p_A^2 b_2 a_3}{r - p_A^2 b_2 a_2} \tag{A.4}$$

where p_A is the fraction of A reacted; b_2 is the mole fraction of B groups located on the difunctional B-molecules; a_3 is the mole fraction of A groups located on the trifunctional A-molecules; a_2 is the mole fraction of A groups located on the difunctional A-molecules; and r is the stoichiometric ratio, which is defined as p_A/p_B, where p_B is the fraction of B reacted. For our sample, $r = 1$ and $b_2 = 1$ because all the B groups are located on B_2. We also assume complete conversion, so $p_A = 1$. The branching coefficient then has a value of 1. We also need to determine the mass of polymer per mole of A, W[21]:

$$W = a_3E_{A_3} + a_2E_{A_2} + a_1E_{A_1} + rb_2E_{B_2} + rb_1E_{B_1} \tag{A.5}$$

where the E's are the equivalent weights of the reactants identified by the subscripts, a_1 is the mole fraction of A groups located on the monofunctional A-molecules, and b_1 is the mole fraction of B groups located on the monofunctional B-molecules. For our sample, $a_1 = b_1 = 0$, given that there are no monofunctional reactants. The crosslink density can then be determined by[21]

$$\nu = \frac{a_3\rho}{2W}\left(\frac{2\alpha - 1}{\alpha}\right)^3 \tag{A.6}$$

If we substitute eqs. (A.4) and (A.5) into eq. (A.6) with all our assumptions, we obtain

$$\nu = \frac{a_3\rho}{2(a_3E_{A_3} + a_2E_{A_2} + b_2E_{B_2})} \tag{A.7}$$

Equation (A.7) can be further simplified by setting

$$a_3 = 3n_{A_3}/n_A \qquad E_{A_3} = M_{A_3}/3$$
$$a_2 = 2n_{A_2}/n_A \qquad E_{A_2} = M_{A_2}/2$$
$$b_2 = 2n_{B_2}/n_B \qquad E_{B_2} = M_{B_2}/2$$

where n_A is the number of moles of A groups and n_B is the number of moles of B groups. Because this is a stoichiometric sample, $n_B = n_A = 2n_{B_2}$ and eq. (A.7) becomes equal to eq. (A.3). Therefore, the Marsh et al. method is equivalent to the Scanlan method for this sample.

Method of Miller and Macosko

One parameter we need to determine is $P(F_A^{out})$, the probability of finding a finite chain looking out from A_f, where A_f is a reactant containing A groups with functionality f. $P(F_A^{out})$ can be deter-

mined from eq. (22) of Reference 24 for our sample:

$$P(F_A^{out})^2 + \frac{a_2 r p_A^2 - 1}{a_3 r p_A^2} P(F_A^{out}) + \frac{1 - r p_A^2}{a_3 r p_A^2} = 0 \quad (A.8)$$

where r is now defined as p_B/p_A. For our stoichiometric sample ($r = 1$) with full conversion ($p_A = 1$), $P(F_A^{out}) = 0$. Another parameter we need to determine is $P(X_{m,f})$, the probability that an f functional reactant has reacted m times. $P(X_{m,f})$ can be calculated from eq. (45) of Reference 24 for our sample:

$$P(X_{3,3}) = \binom{3}{3}[1 - P(F_A^{out})]^3 = 1 \quad (A.9)$$

where $\binom{x}{y}$ equals $x!/y!(x - y)!$ and is defined as the number of combinations of x items taken y at a time. The probability that A_3 has reacted three times is equal to 1. To determine the crosslink density, we first need to determine the moles of chain ends bound to network junctions, from which we can determine the moles of elastically effective chains. For our stoichiometric sample at full conversion, the total moles of chain ends bound to network junctions is just $3(n_{A_3})P(X_{3,3}) = 3(n_{A_3})(1) = 3(n_{A_3})$. One elastically effective chain has two chain ends. Therefore, the total moles of elastically effective chains is $3(n_{A_3})P(X_{3,3})/2$. The crosslink density is then defined as the total moles of elastically effective chains divided by the volume of the fully cured polymer:

$$\nu = \frac{3 n_{A_3} P(X_{3,3}) \rho}{2(M_{B_2} n_{B_2} + M_{A_2} n_{A_2} + M_{A_3} n_{A_3})} \quad (A.10)$$

Substituting in the appropriate values for the 40 mol % triol sample, we obtained a crosslink density of 3.02×10^{-4} mol/cm^3.

REFERENCES

1. Petrovic, Z. S.; Ferguson, J. Prog Polym Sci 1991, 16, 695.
2. Smith, T. L.; Magnusson, A. B. J Polym Sci 1960, 42, 391.
3. Smith, T. L.; Magnusson, A. B. J Appl Polym Sci 1961, 5, 218.
4. Haska, S. B.; Bayramli, E.; Pekel, F.; Ozkar, S. J Appl Polym Sci 1997, 64, 2347.
5. Petrovic, Z. S.; Ilavsky, M.; Dusek, K.; Vidakovic, M.; Javni, I.; Banjanin, B. J Appl Polym Sci 1991, 42, 391.
6. Kothandaraman, H.; Venkatarao, K.; Thanoo, B. C. Polym J 1989, 21, 829.
7. Kothandaraman, H.; Venkatarao, K.; Thanoo, B. C. J Appl Polym Sci 1990, 39, 943.
8. Consaga, J. P.; French, D. M. J Appl Polym Sci 1971, 15, 2941.
9. Kontou, E.; Spathis, G.; Niaounakis, M.; Kefalas, V. Colloid Polym Sci 1990, 268, 636.
10. Paulmer, R. D. A.; Shah, C. S.; Patni, M. J.; Pandya, M. V. J Appl Polym Sci 1991, 43, 1953.
11. Jung, H. C.; Kang, S. J.; Kim, W. N.; Lee, Y.-B.; Choe, K. H.; Hong, S.-H.; Kim, S.-B. J Appl Polym Sci 2000, 78, 624.
12. Desai, S.; Thakore, I. M.; Sarawade, B. D.; Devi, S. Eur Polym J 2000, 36, 711.
13. Spirkova, M.; Matejka, L.; Hlavata, D.; Meissner, B.; Pytela, J. J Appl Polym Sci 2000, 77, 381.
14. Nielsen, L. E. J Macromol Sci Rev Macromol Chem 1969, C3, 69.
15. Stutz, H.; Illers, K.-H.; Mertes, J. J Polym Sci Part B Polym Phys 1990, 28, 1483.
16. Shefer, A.; Gottlieb, M. Macromolecules 1992, 25, 4036.
17. Hale, A.; Macosko, C. W.; Bair, H. E. Macromolecules 1991, 24, 2610.
18. Nielsen, L. E. Mechanical Properties of Polymers and Composites, Vol. 1; Marcel Dekker: New York, 1974.
19. Scanlan, J. J Polym Sci 1960, 43, 501.
20. Hill, L. W. Prog Org Coat 1997, 31, 235.
21. Marsh, H. E., Jr.; Chung, S. Y.; Hsu, G. C.; Wallace, C. J. in Chemistry and Properties of Crosslinked Polymers; Labana, S. S., Ed.; Academic Press: New York, 1977; pp 341–374.
22. Sekkar, V.; Rao, M. R.; Krishnamurthy, V. N.; Jain, S. R. J Appl Polym Sci 1996, 62, 2317.
23. Sekkar, V.; Bhagawan, S. S.; Prabhakaran, N.; Rao, M. R.; Ninan, K. N. Polymer 2000, 41, 6773.
24. Miller, D. R.; Macosko, C. W. Macromolecules 1976, 9, 206.
25. Queslel, J. P.; Mark, J. E. Adv Polym Sci 1984, 65, 135.
26. Dossin, L. M.; Graessley, W. W. Macromolecules 1979, 12, 123.
27. Graessley, W. W. Macromolecules 1975, 8, 186.
28. Gottlieb, M.; Macosko, C. W.; Benjamin, G. S.; Meyers, K. O.; Merrill, E. W. Macromolecules 1981, 14, 1039.
29. Ward, I. M. Mechanical Properties of Solid Polymers, 2nd ed.; Wiley: New York, 1983.
30. Scanlan, J. C.; Webster, D. C.; Crain, A. L. in Film Formation in Waterborne Coatings; Provder, T.; Winnik, M. A.; Urban, M. W., Eds.; ACS Symposium Series 648; American Chemical Society: Washington, DC, 1996; p 222.
31. Hill, L. W.; Kozlowski, K. J Coat Tech 1987, 59, 63.
32. Hill, L. W. J Coat Tech 1992, 64, 29.